Reactions of Bis(nitro)[α,α,α,α-*meso*-tetrakis(*o*-pivalamidophenyl)porphinato]iron(III) with 2,3,5,6-Tetrafluorothiophenol and 2,3,5,6-Tetrafluorothiophenolate. EPR and Mössbauer Spectra and Molecular Structures

Habib Nasri,[1] Kenneth J. Haller,[1] Yaning Wang,[2] Boi Hanh Huynh,*[,2] and W. Robert Scheidt*[,1]

Department of Chemistry and Biochemistry, University of Notre Dame, Notre Dame, Indiana 46556, and Department of Physics, Emory University, Atlanta, Georgia 30322

Received January 29, 1992

The reactions of the bis(nitro)iron(III) picket fence porphyrin derivative $[K(18C6)(H_2O)][Fe(NO_2)_2(TpivPP)]$ with thiols and thiolates have been examined. The reaction of $[K(18C6)(H_2O)][Fe(NO_2)_2(TpivPP)]$ with an excess of potassium 2,3,5,6-tetrafluorothiophenolate (solubilized with 18-crown-6) yields crystalline $[K(18C6)][Fe(NO_2)(SC_6HF_4)(TpivPP)]$. This species has been characterized by UV-vis, IR, EPR, and Mössbauer spectroscopy and an X-ray diffraction study. The solid-state EPR spectrum is low-spin rhombic with $g_1 = 2.40$, $g_2 = 2.30$, and $g_3 = 1.91$ (77 K). Frozen-solution spectra are virtually identical. Mössbauer spectra are reported. The isomer shift, δ, is 0.22 mm/s, and the quadrupole doublet splitting, ΔE_q, is 2.12 mm/s at 295 K. The X-ray structure of $[Fe(NO_2)(SC_6HF_4)(TpivPP)]^-$ shows that the nitro group is bonded to iron on the pocket side of the porphyrin. The 2,3,5,6-tetrafluorothiophenolate (SC_6HF_4) is coordinated to the iron on the open face. The equatorial bonds average to 1.980 (9) Å, the axial Fe–N(NO_2) distance is 1.990 (7) Å, and the Fe–S(SC_6HF_4) distance is 2.277 (2) Å. The $[K(18C6)]^+$ ion is also coordinated to a carbonyl oxygen atom of a porphyrin picket; the seven-coordinate potassium ion is displaced 0.55 Å from the crown oxygen plane. Reaction of $[K(18C6)(H_2O)][Fe(NO_2)_2(TpivPP)]$ with thiols leads to a formal two-electron reduction to yield ferrous nitrosyl complexes as shown both by EPR spectroscopy (g = 2.11, 2.07, 2.01) and a single-crystal structure determination. The crystal structure shows that the solid-state species obtained has the formulation $[Fe(NO)(TpivPP)][K(NO_2)(18C6)]\cdot{}^1/_2C_6H_5Cl$. The [Fe(NO)(TpivPP)] species has the nitrosyl group in the pocket defined by the four pickets and has two (disordered) positions of the nitrosyl oxygen atom. The average value of the Fe–N_p distance is 1.981 (26) Å, and the axial Fe–N(NO) distance is 1.716 (15) Å. The presence of 18-crown-6 in the cell results from the cocrystallization of a $[K(18C6)]^+$ complex. The potassium ion is also bonded to a nitrite ion through both oxygen atoms; the eight-coordinate potassium ion is displaced 0.77 Å out of the crown oxygen atom plane. Crystal data for $[K(18C6)][Fe(NO_2)(SC_6HF_4)(TpivPP)]\cdot 2C_6H_6\cdot C_5H_{12}$: a = 29.363 (1) Å, b = 24.596 (2) Å, c = 13.379 (6) Å, β = 95.68 (8)°, monoclinic, space group $P2_1/a$, V = 9615.0 Å^3, Z = 4, $FeKSF_4O_{12}N_9C_{105}H_{119}$, 9861 observed data, final data/variable = 8.1, R_1 = 0.089, R_2 = 0.107, all observations at 294 K. Crystal data for $[Fe(NO)(TpivPP)][K(NO_2)(18C6)]\cdot{}^1/_2C_6H_5Cl$: a = 13.157 (4) Å, b = 19.481 (8) Å, c = 30.784 (13) Å, β = 97.25 (16)°, monoclinic, space group $P2_1/n$, V = 7827.2 Å^3, Z = 4, $FeKCl_{0.5}O_{13}N_{10}C_{79}H_{66.5}$, 3594 observed data, final data/variable = 7.1, R_1 = 0.098, R_2 = 0.081, all observations at 294 K.

Introduction

The nitrite ion/iron porphyrinate system is an interesting one both because of the exceptionally strong bonding interactions in the pair and the chemical properties of the system. In previous work, we have shown that the N-bonded nitrite ion coordinates as a strong π-accepting ligand to iron.[3,4] Indeed, it is so strong that a single nitrite ligand yields the low-spin iron(II) derivative $[Fe(NO_2)(TpivPP)]^-$.[5,6] Moreover, the coordination of nitrite to unprotected ion(III) porphyrinates leads to significant reactivity of the coordinated ligand.[7] Finally, the nitrite ion interacts with a number of hemoprotein derivatives with varying chemistries, ranging from meat-curing processes[8] to assimilatory[9] and dissimilatory[10] nitrite reduction catalysis. The nature of all the ligands in these species is generally not yet clear, although the assimilatory nitrite reductases seem to be unusual in at least two ways. First, these systems contain a novel isobacteriochlorin prosthetic group (siroheme[11]), and second, the heme iron appears to interact with an Fe_4S_4 cluster,[12] presumably via a bridged sulfide link.

In this paper, we report on the reactions of potential sulfur ligands with nitrite-coordinated iron(III) porphyrinate derivatives. *Thiolates* react with $[Fe(NO_2)_2(TpivPP)]$ to yield to mixed-ligand nitro/thiolato complex, while *thiols* yield a reduction

(1) University of Notre Dame.
(2) Emory University.
(3) Nasri, H.; Goodwin, J. A.; Scheidt, W. R. *Inorg. Chem.* **1990**, *29*, 185.
(4) Nasri, H.; Wang, Y.; Huynh, B. H.; Walker, F. A.; Scheidt, W. R. *Inorg. Chem.* **1991**, *30*, 1483.
(5) Nasri, H.; Wang, Y.; Huynh, B. H.; Scheidt, W. R. *J. Am. Chem. Soc.* **1991**, *113*, 717.
(6) Abbreviations used in this paper: H_2TpivPP, picket fence porphyrin; H_2OEP, octaethylporphyrin; H_2PP IX DME, protoporphyrin IX dimethyl ester; H_2TPP, *meso*-tetraphenylporphyrin; 18C6, 18-crown-6; SC_6HF_4, 2,3,5,6-tetrafluorothiophenolate; Py, pyridine; HIm, imidazole; 2-PhIm, 2-phenylimidazole; SPh, benzenethiolate; SPhBr, 4-bromobenzenethiolate; $SPhNO_2$, 4-nitrobenzenethiolate; SEt, ethanethiolate; N_p, porphinato nitrogen; EPR, electron paramagnetic resonance.
(7) Finnegan, M. G.; Lappin, A. G.; Scheidt, W. R. *Inorg. Chem.* **1990**, *29*, 181.
(8) Giddings, G. G. *J. Food Sci.* **1977**, *42*, 288. Cassens, R. G.; Greaser, M. L.; Ito, T.; Lee, M. *Food Technol.* **1979**, *33*, 46.
(9) Vegas, J. M.; Kamin, H. *J. Biol. Chem.* **1977**, *252*, 896. Coleman, K. J.; Cornish-Bowden, A.; Cole, J. A. *Biochem. J.* **1978**, *175*, 483.
(10) Firestone, M. K.; Firestone, R. B.; Tiedje, J. M. *Biochem. Biophys. Res. Commun.* **1979**, *61*, 10. Johnson, M. K.; Thomson, A. J.; Walsh, T. A.; Barber, D.; Greenwood, C. *Biochem. J.* **1980**, *189*, 285.
(11) Murphy, M. J.; Siegel, L. M.; Kamin, H. *J. Biol. Chem.* **1973**, *248*, 251. Scott, A. I.; Irwin, A. J.; Siegel, L. M. *J. Am. Chem. Soc.* **1978**, *100*, 316.
(12) Cammack, R.; Hucklesby, D.; Hewitt, E. J. *J. Biochem.* **1978**, *171*, 519. Crowe, B. A.; Patil, D. S.; Cammack, R. *Eur. J. Biochem.* **1983**, *137*, 185. Moura, I.; LeGall, J.; Lino, A. R.; Peck, H. D.; Fauque, G.; Xavier, A. V.; DerVartanian, D. V.; Moura, J. J. G.; Huynh, B. H. *J. Am. Chem. Soc.* **1988**, *110*, 1075.

0020-1669/92/1331-3459$03.00/0

product, a ferrous nitrosyl derivative. The characterization of these products is the subject of this paper.

Experimental Section

General Information. UV–vis spectra were recorded on a Perkin-Elmer Lambda 4C spectrometer and IR spectra on a Perkin-Elmer Model 883 spectrometer in KBr pellets. EPR spectra were obtained at 77 K on a Varian E-line spectrometer operating at X-band frequency. Both the strong- and weak-field Mössbauer spectrometers, operating in a constant-acceleration mode with a transmission arrangement, have been described elsewhere.[13] The zero velocities of the Mössbauer spectra are referred to the centroid of the room-temperature spectrum of a metallic iron foil. A sample of $[K(18C6)][Fe(NO_2)(SC_6HF_4)(TpivPP)]\cdot 2C_6H_6\cdot C_5H_{12}$ for Mössbauer spectroscopy was prepared by immobilization of the crystalline material (crystals not ground) in paraffin wax (mp 78 °C) in the drybox.

The free base $\alpha,\alpha,\alpha,\alpha$-*meso*-tetrakis(*o*-pivalamidophenyl)porphyrin ($H_2TpivPP$) and the corresponding chloro and triflate iron(III) derivatives were synthesized by literature methods.[14,15] The potassium salt of 2,3,5,6-tetrafluorothiophenol was prepared in dry ethanol. This solvent was distilled twice over CaH_2. KOH (1.1 g, 20 mmol) was first ground, dried for 1 h under vacuum, and then dissolved in dry ethanol (20 mL). 2,3,5,6-Tetrafluorothiophenol (5 g, 25 mmol) was added to this solution in small portions. The pale yellow solution was stirred for about 1 h, and then 10 mL of dry ether (distilled over Na) was added. The KSC_6HF_4 salt started to precipitate. This precipitation was completed after adding an additional 10 mL of ether. The white salt was washed with 25 mL of dry pentane, dried overnight under vacuum, and stored under argon. The purity of the potassium thiolate was checked by IR spectroscopy.

Preparation of $[K(18C6)][Fe(NO_2)(SC_6HF_4)(TpivPP)]\cdot 2C_6H_6\cdot C_5H_{12}$. $[K(18C6)(H_2O)][Fe(NO_2)_2(TpivPP)]$[3] (100 mg, 0.07 mmol) was stirred for about 30 min in 20 mL of benzene (dried by distillation over Na/benzophenone). To this deep red solution were added 92.4 mg (0.35 mmol) of 18-crown-6 and 154 mg (0.80 mmol) of potassium 2,3,5,6-tetrafluorothiophenolate. The resulting red-green solution was filtered, and single crystals of the compound were prepared by slow diffusion of pentane into the benzene solution. The resulting crystalline material was washed with portions of distilled water to remove excess ligand and 18-crown-6 and then washed with several portions of dry pentane. Typical yields were 60–75%. EPR (C_6H_5Cl solution, 77 K): $g_1 = 2.39$, $g_2 = 2.30$, $g_3 = 1.90$. EPR (solid state, 77 K): $g_1 = 2.40$, $g_2 = 2.30$, $g_3 = 1.91$. UV–vis spectra were taken in the solid-state to avoid problems with competing equilibria in solution. UV–vis (solid state), λ_{max}, nm: 382, 450, 557, 588. IR (KBr pellet), $\nu(NO_2)$, cm^{-1}: 1352 (m).

Preparation of $[Fe(NO)(TpivPP)][K(NO_2)(18C6)]\cdot {}^1/_2C_6H_5Cl$. $[K(18C6)(H_2O)][Fe(NO_2)_2(TpivPP)]$[3] (100 mg, 0.07 mmol) was dissolved in 15 mL of chlorobenzene (dried by distillation over P_2O_5), and 0.1 mL of 2,3,5,6-tetrafluorothiophenol (Aldrich, used without further purification) was added. The color of the solution immediately changed from deep red to light red. Single crystals of the complex were prepared by slow diffusion of dry pentane into the chlorobenzene solution. The resulting crystalline material was washed with portions of dry pentane. Typical yields were about 70%. UV–vis (C_6H_5Cl), λ_{max}, nm (log ϵ): 412 (5.23), 476 (4.56) (sh), 539 (4.42). IR (KBr pellet), $\nu(NO)$, cm^{-1}: ~1665 (s, picket carbonyl as shoulder at ~1675). EPR (chlorobenzene 77 K): $g_1 = 2.11$, $g_2 = 2.07$, $a_2(^{14}N) = 18$ G, $g_3 = 2.01$, $a_3(^{14}N) = 17$ G.

X-ray Diffraction Studies. $[K(18C6)][Fe(NO_2)(SC_6HF_4)(TpivPP)]\cdot 2C_6H_6\cdot C_5H_{12}$. A suitable dark purple, crystalline plate with approximate dimensions 0.67 × 0.57 × 0.10 mm was examined with graphite-monochromated Cu Kα radiation on an Enraf-Nonius CAD4 diffractometer at 294 K. Final cell constants and space group are reported in Table I. Intensity data were measured with θ–2θ scans at a constant scan rate of 3°/min (in θ). The intensity data were reduced with the Blessing[16] data reduction programs with corrections for Lorentz and polarization and were also corrected for absorption by an empirical (ψ scans) absorption correction ($\mu = 2.44$ mm^{-1}). Data were collected to a maximum 2θ of 138.28°. A total of 9861 reflections having $(\sin\theta)/\lambda < 0.602$ $Å^{-1}$ and $F_o \geq 3.0\sigma(F_o)$ were taken as observed. Complete crystallographic details, including data collection parameters, are given as supplementary material in Table SI.

Table I. Crystallographic Data for $[K(18C6)][Fe(NO_2)(SC_6HF_4)(TpivPP)]\cdot 2C_6H_6\cdot C_5H_{12}$ and $[K(NO_2)(18C6)][Fe(NO)(TpivPP)]\cdot {}^1/_2C_6H_5Cl$

	$[Fe(NO_2)(SC_6HF_4)(TpivPP)]^-$	$[Fe(NO)(TpivPP)][K(NO_2)(18C6)]$
formula	$FeKSF_4O_{12}N_9C_{105}H_{119}$	$FeKCl_{0.5}O_{13}N_{10}C_{79}H_{66.5}$
fw	1902.17	1476.64
space group	$P2_1/a$	$P2_1/n$
T, K	294	294
a, Å	29.363 (1)	13.157 (4)
b, Å	24.596 (2)	19.481 (8)
c, Å	13.379 (1)	30.784 (13)
β, deg	95.68 (8)	97.25 (16)
V, $Å^3$	9615.0	7827.2
Z	4	4
scan technique	θ–2θ	θ–2θ
cryst dimens, mm	0.67 × 0.57 × 0.10	0.34 × 0.25 × 0.21
2θ limits, deg	4.0–136.3	4.0–50.7
radiation	Cu Kα	Mo Kα
μ, mm^{-1}	2.44	0.32
R_1	0.089	0.098
R_2	0.107	0.091

The structure was solved by direct methods (MULTAN[17] and DIRDIF[18]). The crystal contains three solvent molecules: two of benzene and one of pentane. The first benzene molecule was readily found and refined; the remaining two solvent molecules were much more diffuse in difference Fourier maps. The second benzene was assigned atomic occupancies of 0.5; a reasonable geometry was obtained. The last solvate molecule was eventually identified as a pentane molecule. A careful examination of the solvent regions[19] led to the identification of a partially occupied pentane molecule (50%) with a final assignment in which the end atomic positions (C(79)) are disordered into two positions (occupancies fixed at 0.3 and 0.2). There are, as a result, six atomic positions for the five atoms of a pentane molecule. After isotropic full-matrix least-squares refinement was carried to convergence, a difference Fourier map suggested possible locations for all hydrogen atoms of the 18C6 and the porphyrin except those of the *tert*-butyl groups of the pickets and the solvates. Hydrogen atoms were included in subsequent cycles of least-squares refinement as fixed, idealized contributors as before. Final cycles of full-matrix least-squares refinement used anisotropic temperature factors for all heavy atoms except two methyl carbons of pivalamido groups (C(22), C(33)) and the carbon atoms of the pentane. At convergence, $R_1 = 0.089$ and $R_2 = 0.107$, the error of fit was 1.87 and the final data/variable ratio was 8.1. A final difference Fourier map was judged to be significantly free of features, with the largest peak having a height of 0.74 e/$Å^3$. Final atomic coordinates are listed in Table II. Anisotropic thermal parameters for all heavy atoms and the fixed hydrogen atom coordinates are available as supplementary material (Tables SII and SIII).

$[Fe(NO)(TpivPP)][K(NO_2)(18C6)]\cdot {}^1/_2C_6H_5Cl$. A dark purple crystal with approximate dimensions 0.34 × 0.25 × 0.21 mm was examined with graphite-monochromated Mo Kα radiation on an Enraf-Nonius CAD4 diffractometer at 294 K. Final cell constants and space group are reported in Table I. Intensity data were collected and reduced as before, except that no absorption correction was applied ($\mu = 0.32$ mm^{-1}). A total of 3594 reflections having $(\sin\theta)/\lambda < 0.602$ $Å^{-1}$ and $F_o \geq 3.0\sigma(F_o)$ were

(13) Kretchmar, S. A.; Teixeira, M.; Huynh, B. H.; Raymond, K. N. *Biol. Met.* **1988**, *1*, 26.
(14) Collman, J. P.; Gagne, R. R.; Halbert, T. R.; Lang, G.; Robinson, W. T. *J. Am. Chem. Soc.* **1975**, *97*, 1427.
(15) Gismelseed, A.; Bominaar, E. L.; Bill, E.; Trautwein, A. X.; Nasri, H.; Doppelt, P.; Mandon, D.; Fischer, J.; Weiss, R. *Inorg. Chem.* **1990**, *29*, 2741.
(16) Blessing, R. H. *Crystallogr. Rev.* **1987**, *1*, 3.
(17) Programs used in this study included local modifications of Main, Hull, Lessinger, Germain, Declerq, and Woolfson's MULTAN, Jacobson's ALLS, Zalkin's FORDAP, Busing and Levy's ORFFE, and Johnson's ORTEP2. Atomic form factors were from: Cromer, D. T.; Mann, J. B. *Acta Crystallogr., Sect. A* **1968**, *A24*, 321. Real and imaginary corrections for anomalous dispersion in the form factor of the iron, sulfur, chlorine, and potassium atoms were from: Cromer, D. T.; Liberman, D. J. *J. Chem. Phys.* **1970**, *53*, 1891. Scattering factors for hydrogen were from: Stewart, R. F.; Davidson, E. R.; Simpson, W. T. *Ibid.* **1965**, *42*, 3175. All calculations were performed on a VAX 3200 computer.
(18) DIRDIF: Beurskens, P. T.; Bosman, W. P.; Doesburg, H. M.; Gould, R. O.; van den Hark, Th. E. M.; Prick, P. A. J.; Noordik, J. H.; Beurskens, G.; Parthasarathi, V.; Bruins Slot, H. J.; Haltiwanger, R. C.; Strumpel, M.; Smits, J. M. Technical Report 1984/1; Crystallography Laboratory: Nijmegen, The Netherlands, 1984.
(19) The program CAVITY[20] was used to examine and compare the cavity shapes for all three solvent molecules; the shape of the pentane cavity was inconsistent with the presence of a *planar, six-membered* ring.
(20) Basso, R.; Della Giusta, A. *J. Appl. Crystallogr.* **1977**, *10*, 496.

Table II. Fractional Coordinates of $[K(18C6)][Fe(NO_2)(C_6HF_4S)(TpivPP)]\cdot 2C_6H_6\cdot C_5H_{12}$[a]

atom	x	y	z	atom	x	y	z
Fe	0.66584 (3)	0.22921 (4)	0.99258 (7)	C(16)	0.8886 (3)	0.2564 (4)	0.8301 (9)
K	0.84461 (5)	0.48850 (7)	0.56657 (12)	C(17)	0.84631 (28)	0.2427 (4)	0.8621 (8)
S	0.68028 (5)	0.14097 (7)	1.03628 (15)	C(18)	0.77430 (27)	0.4137 (3)	0.7561 (6)
F(1)	0.72590 (20)	0.09990 (24)	0.8617 (4)	C(19)	0.7323 (3)	0.4453 (4)	0.7748 (8)
F(2)	0.81452 (26)	0.0890 (3)	0.8463 (6)	C(20)	0.7393 (9)	0.4755 (16)	0.8628 (24)
F(3)	0.84615 (23)	0.1402 (3)	1.1835 (7)	C(21)	0.6922 (6)	0.4138 (8)	0.767 (3)
F(4)	0.75707 (21)	0.15280 (24)	1.1992 (4)	C(23)	0.60527 (22)	0.1404 (3)	0.6805 (5)
O(1)	0.6762 (3)	0.4414 (4)	1.4077 (6)	C(24)	0.58661 (25)	0.1663 (4)	0.5925 (6)
O(2)	0.80249 (21)	0.43173 (25)	0.7046 (5)	C(25)	0.5691 (3)	0.1342 (5)	0.5100 (6)
O(3)	0.5370 (4)	0.2415 (5)	0.4571 (7)	C(26)	0.5701 (3)	0.0790 (5)	0.5184 (8)
O(4)	0.42925 (24)	0.3462 (4)	1.0077 (8)	C(27)	0.5875 (3)	0.0526 (4)	0.6038 (8)
O(5)	0.92384 (21)	0.42803 (28)	0.6326 (5)	C(28)	0.60472 (28)	0.0847 (4)	0.6849 (7)
O(6)	0.90985 (20)	0.52900 (27)	0.7251 (4)	C(29)	0.5636 (4)	0.2587 (6)	0.5281 (7)
O(7)	0.83150 (20)	0.58824 (23)	0.6542 (4)	C(30)	0.5753 (8)	0.3198 (6)	0.5515 (10)
O(8)	0.79044 (19)	0.56959 (25)	0.4635 (5)	C(31)	0.5466 (13)	0.3303 (9)	0.6397 (19)
O(9)	0.80412 (22)	0.46996 (28)	0.3715 (5)	C(32)	0.6249 (10)	0.3300 (10)	0.5810 (26)
O(10)	0.88489 (24)	0.41257 (25)	0.4339 (5)	C(34)	0.51407 (20)	0.21722 (29)	1.1223 (5)
O(11)	0.65450 (27)	0.34243 (28)	1.0061 (6)	C(35)	0.48222 (22)	0.2578 (3)	1.0983 (6)
O(12)	0.63173 (26)	0.3131 (3)	0.8614 (6)	C(36)	0.43989 (26)	0.2557 (4)	1.1383 (8)
N(1)	0.64165 (16)	0.24238 (20)	1.1225 (4)	C(37)	0.43049 (29)	0.2145 (5)	1.1988 (8)
N(2)	0.72645 (16)	0.25766 (20)	1.0471 (4)	C(38)	0.4614 (3)	0.1735 (4)	1.2242 (7)
N(3)	0.68966 (16)	0.21885 (22)	0.8605 (4)	C(39)	0.50382 (24)	0.1755 (3)	1.1836 (6)
N(4)	0.60441 (16)	0.20338 (23)	0.9377 (4)	C(40)	0.46897 (26)	0.3411 (4)	0.9928 (7)
N(5)	0.69265 (24)	0.37517 (29)	1.3009 (5)	C(41)	0.49128 (29)	0.3793 (4)	0.9248 (8)
N(6)	0.77818 (19)	0.36414 (25)	0.7996 (5)	C(42)	0.5416 (5)	0.3669 (8)	0.9108 (16)
N(7)	0.58678 (28)	0.2226 (4)	0.5905 (5)	C(43)	0.4632 (6)	0.3767 (8)	0.8178 (13)
N(8)	0.49392 (21)	0.3001 (3)	1.0360 (6)	C(44)	0.4850 (10)	0.4365 (7)	0.9583 (17)
N(9)	0.64846 (20)	0.30455 (27)	0.9502 (5)	C(45)	0.9555 (4)	0.4530 (5)	0.7086 (11)
C(a1)	0.59662 (18)	0.23642 (26)	1.1484 (4)	C(46)	0.9296 (4)	0.4841 (5)	0.7776 (9)
C(a2)	0.66640 (20)	0.25794 (26)	1.2109 (5)	C(47)	0.8857 (3)	0.5637 (5)	0.7861 (7)
C(a3)	0.73969 (20)	0.27308 (27)	1.1444 (5)	C(48)	0.8662 (3)	0.6089 (4)	0.7258 (6)
C(a4)	0.76381 (19)	0.26988 (28)	0.9936 (5)	C(49)	0.8099 (3)	0.6308 (4)	0.5966 (8)
C(a5)	0.73133 (21)	0.23529 (28)	0.8305 (5)	C(50)	0.7716 (3)	0.6064 (4)	0.5290 (8)
C(a6)	0.66743 (22)	0.1924 (3)	0.7787 (5)	C(51)	0.7573 (3)	0.5457 (5)	0.3948 (9)
C(a7)	0.59349 (20)	0.17964 (29)	0.8452 (5)	C(52)	0.7801 (4)	0.5132 (5)	0.3218 (8)
C(a8)	0.56419 (20)	0.20278 (29)	0.9856 (5)	C(53)	0.8269 (4)	0.4385 (6)	0.3034 (9)
C(b1)	0.59451 (22)	0.2492 (3)	1.2516 (5)	C(54)	0.8501 (4)	0.3922 (5)	0.3584 (10)
C(b2)	0.63702 (23)	0.26086 (29)	1.2911 (5)	C(55)	0.9086 (5)	0.3711 (5)	0.4903 (11)
C(b3)	0.78567 (21)	0.2940 (3)	1.1528 (5)	C(56)	0.9448 (4)	0.3968 (6)	0.5618 (11)
C(b4)	0.80012 (23)	0.2919 (3)	1.0607 (6)	C(57)	0.73819 (21)	0.12955 (26)	1.0288 (5)
C(b5)	0.73465 (25)	0.2189 (4)	0.7292 (5)	C(58)	0.75511 (27)	0.1112 (3)	0.9428 (7)
C(b6)	0.69623 (26)	0.1922 (4)	0.6972 (6)	C(59)	0.8006 (3)	0.1039 (4)	0.9355 (8)
C(b7)	0.54571 (22)	0.1653 (3)	0.8334 (6)	C(60)	0.8320 (3)	0.1136 (4)	1.0153 (12)
C(b8)	0.52783 (21)	0.1805 (3)	0.9177 (6)	C(61)	0.8167 (3)	0.1301 (4)	1.1018 (9)
C(m1)	0.71213 (20)	0.27241 (26)	1.2225 (5)	C(62)	0.77030 (26)	0.1375 (3)	1.1095 (6)
C(m2)	0.76568 (19)	0.26059 (25)	0.8919 (5)	C(63)	0.3597 (5)	0.0060 (6)	0.0337 (11)
C(m3)	0.62301 (22)	0.17219 (29)	0.7730 (5)	C(64)	0.3969 (6)	−0.0242 (6)	0.0562 (9)
C(m4)	0.56040 (19)	0.21974 (26)	1.0816 (5)	C(65)	0.4386 (6)	0.0001 (8)	0.0687 (12)
C(1)	0.73260 (22)	0.29084 (29)	1.3240 (5)	C(66)	0.4432 (7)	0.0534 (8)	0.0562 (14)
C(2)	0.72176 (24)	0.3407 (3)	1.3628 (6)	C(67)	0.4064 (9)	0.0849 (6)	0.0329 (14)
C(3)	0.7396 (3)	0.3559 (4)	1.4605 (6)	C(68)	0.3637 (6)	0.0618 (7)	0.0212 (11)
C(4)	0.7684 (3)	0.3204 (5)	1.5151 (6)	C(69)	−0.1117 (10)	0.1754 (13)	0.4085 (18)
C(5)	0.78070 (28)	0.2715 (4)	1.4769 (6)	C(70)	−0.0899 (11)	0.2079 (11)	0.477 (3)
C(6)	0.76280 (25)	0.2570 (3)	1.3817 (6)	C(71)	−0.1006 (17)	0.1986 (19)	0.5767 (28)
C(7)	0.6705 (3)	0.4207 (4)	1.3246 (8)	C(72)	−0.1251 (14)	0.1564 (26)	0.591 (3)
C(8)	0.6382 (4)	0.4452 (4)	1.2374 (11)	C(73)	−0.1398 (9)	0.1288 (21)	0.522 (3)
C(9)	0.6217 (6)	0.5004 (6)	1.2750 (13)	C(74)	−0.1355 (10)	0.1366 (16)	0.4341 (24)
C(10)	0.6646 (5)	0.4553 (5)	1.1430 (10)	C(75)	−0.0820 (12)	0.0121 (24)	0.239 (5)
C(11)	0.5988 (4)	0.4043 (6)	1.2091 (13)	C(76)	−0.0579 (14)	0.0565 (19)	0.221 (3)
C(12)	0.80968 (21)	0.27628 (29)	0.8497 (5)	C(77)	−0.0241 (17)	0.0576 (27)	0.308 (5)
C(13)	0.81466 (21)	0.32703 (29)	0.8051 (5)	C(78)	−0.0309 (26)	0.0015 (21)	0.364 (5)
C(14)	0.85710 (26)	0.3406 (4)	0.7703 (6)	C(79b)	−0.062 (4)	0.022 (5)	0.398 (6)
C(15)	0.89276 (27)	0.3050 (4)	0.7824 (8)	C(79a)	−0.0792 (23)	−0.009 (3)	0.324 (10)

[a] The estimated standard deviations of the least significant digits are given in parentheses.

taken as observed. Complete crystallographic details, including data collection parameters, are given in Table SI.

The structure was solved by a combination of Patterson[17] and direct methods (DIRDIF[18]). The positions of the two heavy atoms were determined by solving the Patterson map. Most atoms of the porphinato ligand were found with DIRDIF; the remaining atoms were found in subsequent difference Fourier maps. After isotropic full-matrix least-squares refinement was carried to convergence, a difference Fourier map suggested possible locations for almost all hydrogen atoms of the porphyrin except those of the *tert*-butyl groups. These hydrogen atoms were included in subsequent cycles of least-squares refinement as fixed, idealized contributors (C–H = 0.95 Å, N–H = 0.90 Å, and $B(H) = 1.3B(C,N)$). Three significant disorder problems were encountered during the course of refinement. The first concerns the oxygen atom of the nitrosyl group (NO), which is disordered in two positions (with 70% and 30% occupancies). The second disorder problem, which is common to many other picket fence porphyrin structures,[21] involves one methyl group of a pivalamido side chain. Atoms of this group are disordered in two major positions (60% and 40% occupancies). The last disorder problem involves one carbon atom, C(53), of the crown which shows two major positions (60% and 40% occupancies). Final cycles of full-matrix least-squares refinement used anisotropic temperature factors for only 14 heavy atoms.

Table III. Fractional Coordinates for [Fe(NO)(TpivPP)][K(NO_2)(18C6)]·$^1/_2C_6H_5Cl$[a]

atom	x	y	z	atom	x	y	z
Fe	0.05077 (17)	0.15381 (13)	0.05372 (7)	C(7)	−0.1331 (13)	0.3459 (12)	0.2108 (6)
K	−0.1668 (3)	0.20859 (24)	−0.16915 (15)	C(8)	−0.1273 (19)	0.4071 (13)	0.1790 (8)
Cl	0.4229 (10)	0.0453 (7)	0.4103 (4)	C(9)	−0.0285 (23)	0.3943 (15)	0.1563 (9)
O(1)	−0.1602 (12)	0.3533 (7)	0.2460 (4)	C(10a)	−0.2322 (25)	0.4126 (16)	0.1510 (10)
O(2)	0.5218 (11)	0.3616 (6)	0.1624 (5)	C(10b)	−0.148 (4)	0.3890 (25)	0.1292 (16)
O(3)	0.3659 (10)	0.2695 (6)	−0.1138 (5)	C(12)	0.3983 (12)	0.1630 (9)	0.1355 (5)
O(4)	−0.4484 (9)	0.2515 (7)	0.0094 (4)	C(13)	0.4520 (13)	0.2225 (9)	0.1471 (5)
O(5)	−0.249 (4)	0.0631 (19)	−0.1920 (14)	C(14)	0.5521 (13)	0.2172 (9)	0.1708 (5)
O(6)	−0.3818 (16)	0.1707 (15)	−0.1721 (6)	C(15)	0.5869 (12)	0.1535 (10)	0.1830 (5)
O(7)	−0.3403 (15)	0.3146 (12)	−0.1818 (5)	C(16)	0.5336 (14)	0.0965 (9)	0.1726 (5)
O(8)	−0.1205 (26)	0.3539 (14)	−0.1975 (7)	C(17)	0.4361 (12)	0.1005 (9)	0.1484 (5)
O(9)	0.0199 (24)	0.2348 (19)	−0.2164 (8)	C(18)	0.4377 (18)	0.3502 (14)	0.1405 (7)
O(10)	−0.050 (5)	0.100 (4)	−0.2032 (9)	C(19)	0.3670 (18)	0.4071 (12)	0.1203 (7)
O(11)	−0.1504 (11)	0.2502 (7)	−0.0816 (4)	C(20)	0.3308 (16)	0.3926 (11)	0.0707 (7)
O(12)	−0.0069 (9)	0.2457 (7)	−0.1007 (5)	C(21)	0.2703 (17)	0.4096 (11)	0.1453 (7)
O(13a)	0.0880 (17)	0.2914 (12)	0.0550 (7)	C(22)	0.4313 (18)	0.4714 (13)	0.1234 (7)
O(13b)	0.028 (4)	0.2911 (27)	0.0740 (16)	C(23)	0.2018 (11)	0.1062 (8)	−0.0826 (5)
N(1)	0.1061 (8)	0.1589 (6)	0.1152 (4)	C(24)	0.2340 (10)	0.1616 (9)	−0.1076 (5)
N(2)	0.1924 (9)	0.1447 (6)	0.0377 (4)	C(25)	0.2759 (11)	0.1435 (8)	−0.1454 (5)
N(3)	−0.0004 (9)	0.1169 (6)	−0.0057 (4)	C(26)	0.2871 (12)	0.0783 (9)	−0.1584 (5)
N(4)	−0.0889 (9)	0.1423 (6)	0.0706 (4)	C(27)	0.2546 (12)	0.0252 (8)	−0.1341 (5)
N(5)	−0.1155 (10)	0.2818 (8)	0.1958 (4)	C(28)	0.2137 (11)	0.0400 (8)	−0.0955 (5)
N(6)	0.4092 (11)	0.2872 (9)	0.1329 (4)	C(29)	0.2895 (15)	0.2792 (10)	−0.0952 (5)
N(7)	0.2219 (10)	0.2284 (7)	−0.0942 (4)	C(30)	0.2674 (15)	0.3492 (11)	−0.0750 (6)
N(8)	−0.3210 (10)	0.2252 (7)	−0.0306 (4)	C(31)	0.2250 (15)	0.3346 (11)	−0.0303 (7)
N(9)	−0.0506 (14)	0.2616 (10)	−0.0663 (7)	C(32)	0.3629 (18)	0.3922 (12)	−0.0697 (7)
N(10)	0.0449 (11)	0.2412 (8)	0.0468 (5)	C(33)	0.1782 (15)	0.3850 (10)	−0.1054 (6)
C(a1)	0.0499 (11)	0.1654 (8)	0.1516 (5)	C(34)	−0.2901 (12)	0.0997 (8)	−0.0239 (5)
C(a2)	0.2103 (11)	0.1649 (8)	0.1342 (5)	C(40)	−0.3691 (14)	0.2665 (9)	−0.0039 (6)
C(a3)	0.2812 (11)	0.1572 (8)	0.0652 (5)	C(41)	−0.3156 (13)	0.3375 (10)	0.0058 (5)
C(a4)	0.2201 (11)	0.1401 (8)	−0.0042 (5)	C(35)	−0.3237 (12)	0.0320 (8)	−0.0305 (5)
C(a5)	0.0548 (12)	0.1060 (7)	−0.0403 (5)	C(36)	−0.4254 (13)	0.0221 (9)	−0.0535 (5)
C(a6)	−0.1011 (12)	0.1038 (8)	−0.0221 (5)	C(37)	−0.4833 (13)	0.0785 (10)	−0.0666 (5)
C(a7)	−0.1786 (11)	0.1331 (7)	0.0432 (5)	C(38)	−0.4513 (12)	0.1439 (9)	−0.0610 (5)
C(a8)	−0.1177 (11)	0.1528 (8)	0.1116 (5)	C(39)	−0.3530 (12)	0.1531 (9)	−0.0380 (5)
C(b1)	0.1205 (13)	0.1754 (8)	0.1916 (5)	C(42)	−0.2019 (13)	0.3217 (9)	0.0299 (5)
C(b2)	0.2158 (12)	0.1765 (8)	0.1789 (5)	C(43)	−0.3094 (14)	0.3775 (10)	−0.0380 (6)
C(b3)	0.3671 (12)	0.1625 (8)	0.0398 (5)	C(44)	−0.3792 (15)	0.3797 (10)	0.0345 (6)
C(b4)	0.3291 (11)	0.1514 (8)	−0.0019 (5)	C(45)	−0.331 (4)	0.0674 (26)	−0.1981 (14)
C(b5)	−0.0132 (13)	0.0820 (8)	−0.0784 (5)	C(46)	−0.406 (3)	0.1051 (25)	−0.1822 (13)
C(b6)	−0.1101 (13)	0.0815 (8)	0.0669 (5)	C(47)	−0.4423 (26)	0.2206 (23)	−0.1762 (11)
C(b7)	−0.2659 (11)	0.1419 (8)	0.0669 (5)	C(48)	−0.4062 (23)	0.2809 (17)	−0.1572 (9)
C(b8)	−0.2276 (12)	0.1531 (9)	0.1091 (5)	C(49)	−0.278 (3)	0.3749 (18)	−0.1776 (11)
C(m1)	−0.0532 (12)	0.1604 (8)	0.1502 (5)	C(50)	−0.194 (4)	0.3817 (20)	−0.1950 (14)
C(m2)	0.2912 (11)	0.1636 (8)	0.1101 (5)	C(51)	−0.0232 (27)	0.3433 (20)	−0.2131 (9)
C(m3)	0.1586 (12)	0.1181 (7)	−0.0405 (5)	C(52)	0.009 (3)	0.2863 (27)	−0.2122 (14)
C(m4)	−0.1862 (12)	0.1145 (7)	0.0011 (5)	C(53a)	0.039 (8)	0.184 (6)	−0.230 (3)
C(1)	−0.0963 (11)	0.1590 (9)	0.1932 (5)	C(53b)	0.056 (4)	0.1563 (29)	−0.2209 (18)
C(2)	−0.1219 (12)	0.2174 (9)	0.2152 (5)	C(54)	−0.0094 (23)	0.0950 (15)	−0.2301 (9)
C(3)	−0.1614 (11)	0.2085 (9)	0.2556 (5)	C(55)	−0.107 (5)	0.044 (3)	−0.2106 (20)
C(4)	−0.1696 (12)	0.1452 (10)	0.2730 (5)	C(56)	−0.212 (5)	0.0216 (29)	−0.1800 (18)
C(5)	−0.1434 (13)	0.0870 (9)	0.2521 (6)	C(57)	0.4645 (16)	0.0193 (14)	0.4578 (7)
C(11a)	−0.1247 (25)	0.4733 (16)	0.2055 (10)	C(58)	0.4651 (17)	−0.0497 (13)	0.4664 (8)
C(11b)	−0.050 (5)	0.454 (3)	0.2033 (20)	C(59)	0.4935 (16)	0.0666 (11)	0.4912 (9)
C(6)	−0.1058 (13)	0.0967 (9)	0.2121 (6)				

[a] The estimated standard deviations of the least significant digits are given in parentheses.

At convergence, $R_1 = 0.098$ and $R_2 = 0.091$, the error of fit was 2.13 and the final data/variable ratio was 7.0. A final difference Fourier map was judged to be significantly free of features, with the largest peak having a height of 0.57 e/Å^3. Final atomic coordinates are listed in Table III. Isotropic and anisotropic thermal parameters for all heavy atoms and the fixed hydrogen atom coordinates are available as supplementary material (Tables SIV and SV).

Results

The reaction of the bis(nitro) complex with even very deactivated *thiols* such as 2,3,5,6-tetrafluorothiophenol leads to immediate reduction to give a product having solution IR and EPR spectra typical of the well-known ferrous nitrosyl heme derivatives.[22,23] The crystalline product of the reaction was found to have additional features in the IR spectrum suggesting the presence of 18-crown-6. The presence of the crown in the crystalline product suggested some kind of an ionic product. The exact nature of the product could not be deduced from the spectroscopic characterization, but given our earlier observations[7] on the instability of ferric nitrite derivatives, we thought that further characterization was warranted. The nature of the crystalline product was established by a single-crystal X-ray structure determination. This established that the crystals contained [Fe(NO)(TpivPP)][K(NO_2)(18C6)]·$^1/_2C_6H_5Cl$, i.e.,

(21) Ricard, L.; Schappacher, M.; Weiss, R.; Montiel-Montoya, R.; Bill, E.; Gonser, U.; Trautwein, A. X. *Nouv. J. Chim.* **1983**, 7, 405. Schappacher, M.; Ricard, L.; Fischer, J.; Weiss, R.; Bill, E.; Montiel-Montoya, R.; Winkler, H.; Trautwein, A. X. *Eur. J. Biochem.* **1987**, *168*, 419–429.

(22) Scheidt, W. R.; Frisse, M. E. *J. Am. Chem. Soc.* **1975**, *97*, 17.
(23) Wayland, B. B.; Olson, L. W. *J. Am. Chem. Soc.* **1974**, *96*, 6037.

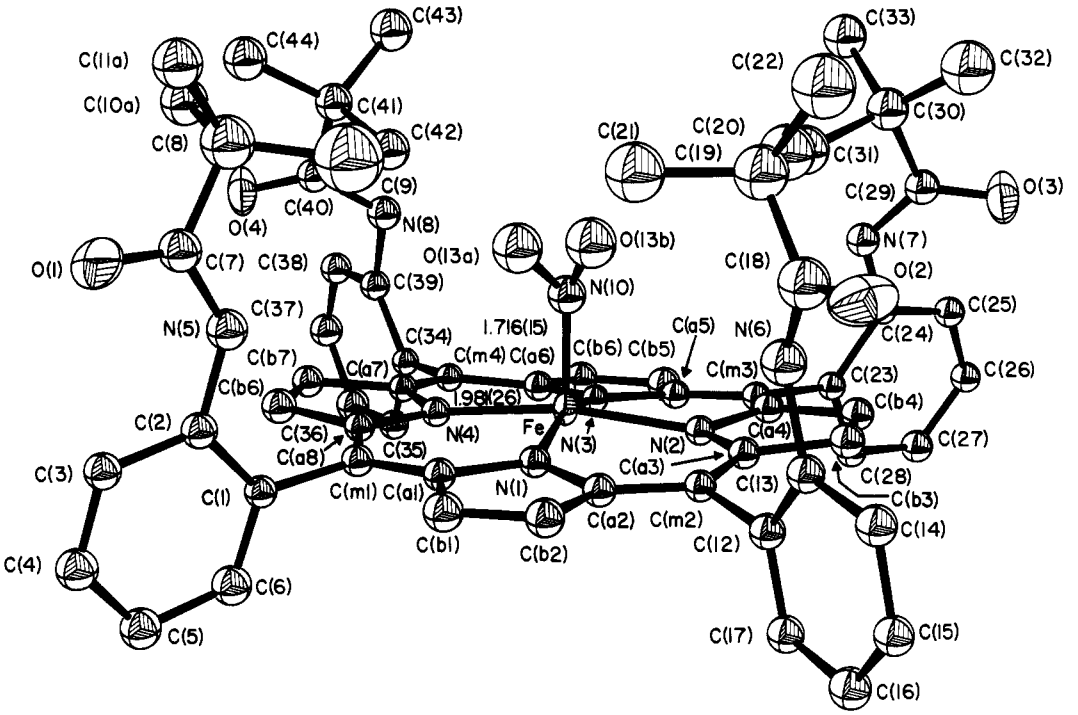

Figure 1. ORTEP diagram illustrating the molecular structure of the [Fe(NO)(TpivPP)] molecule. Both oxygen atoms of the disordered nitrosyl ligand are displayed. The values of the bond distances in the coordination group are also shown. 30% probability surfaces displayed.

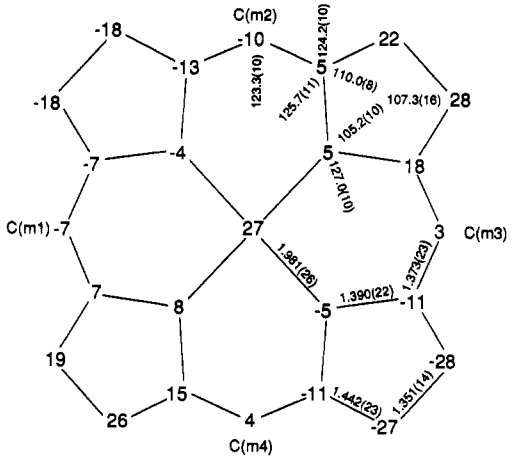

Figure 2. Formal diagram of the porphinato core of [Fe(NO)(TpivPP)] illustrating the displacement of each atom (in units of 0.01 Å) from the mean plane of the 24-atom porphinato core. Positive values of the displacements are toward the axial nitrosyl ligand. Also displayed on the diagram is the averaged value of each type of bond distance and angle in the porphinato core.

a molecule of [Fe(NO)(TpivPP)] and an independent cocrystallized molecule of the nitrite complex of $[K(18C6)]^+$.

The molecular structure of the nitrosyl complex is illustrated in Figure 1. Both of the disordered oxygen positions of the nitrosyl are illustrated. The nitrosyl is coordinated in a bent fashion; the two FeNO angles are 143 and 131°. The angle O(13a)N(10)O(13b) is 49°, and the two N–O bond distances are 1.197 (9) and 1.258 (9) Å. The axial Fe–N(NO) distance is 1.716 (15) Å. Equatorial bond distances ($Fe-N_p$) average to 1.981 (26) Å.[24] Averaged values of the bond distances and bond angles in the porphyrin core are shown in Figure 2. Individual values of bond distances and angles for both molecular species are available as supplementary Tables SVIII and SIX. Also displayed in Figure 2 are the deviations (in units of 0.01 Å) of the crystallographically unique atoms from the mean plane of the 24-atom core. The iron atom is displaced 0.26 Å out of the plane defined by the four nitrogen atoms.

The potassium ion of the 18-crown-6 complex is eight-coordinate with the nitrite ion acting as a bidentate ligand. The average K–O(18C6) distance is 3.018 Å with the shortest being 2.89 Å, and the two K–O distances involving the nitrite ion are 2.798 (14) and 2.877 (14) Å. The potassium ion is displaced 0.77 Å out of the plane defined by the six oxygen atoms toward the nitrite ligand. An ORTEP diagram is available as supplementary material (Figure S1).

The reaction of $[K(18C6)(H_2O)][Fe(NO_2)_2(TpivPP)]$ with crown-solubilized *thiolates* proceeds smoothly with replacement of a nitro ligand, presumably always on the open face of the porphyrin, yielding the mixed-axial-ligand six-coordinate species $[Fe(NO_2)(SR)(TpivPP)]^-$. The reaction appears to be general for all thiolate reagents examined although we have concentrated on reactions with the weakly basic thiolate 2,3,5,6-tetrafluorothiophenolate in order to avoid possible reduction processes. This thiolate yields the crystalline complex $[K(18C6)][Fe(NO_2)(SC_6HF_4)(TpivPP)]\cdot 2C_6H_6\cdot C_5H_{12}$, which has been characterized by UV–vis, EPR, NMR, IR, and Mössbauer spectroscopies and a single-crystal X-ray structure determination.

The molecular structure of this mixed thiolate/nitrite complex is illustrated in Figure 3. The nitro ligand is coordinated in the ligand-binding pocket of the picket fence porphyrin, and the thiolate is on the open face. It is to be noted that all other picket fence iron structures[21,25] with this thiolate are also found to have the thiolate coordinated on the open porphyrin face. The axial $Fe-N(NO_2)$ distance is 1.990 (7) Å, and the Fe–S distance is 2.277 (2) Å. The equatorial $Fe-N_p$ bond distances average to 1.980 (9) Å.[24] Figure 3 also shows the structure of the potassium 18-crown-6 complex. The potassium ion is bonded to the six oxygen atoms of the crown (average K–O(18C6) distance = 2.83 (6) Å, shortest K–O(18C6) distance = 2.76 Å), but it also interacts with a carbonyl group of one of the porphyrin pickets (C–O···K distance is 2.71 Å). Indeed this is the shortest of the seven K–O interactions. The potassium ion is displaced 0.55 Å out of the

(24) The numbers in parentheses following each averaged value is the estimated standard deviation calculated on the assumption that all values are drawn from the same population.

(25) Schappacher, M.; Ricard, L.; Weiss, R.; Montiel-Montoya, R.; Gonser, U.; Bill, E.; Trautwein, A. X. *Inorg. Chim. Acta* **1983**, *78*, L9.

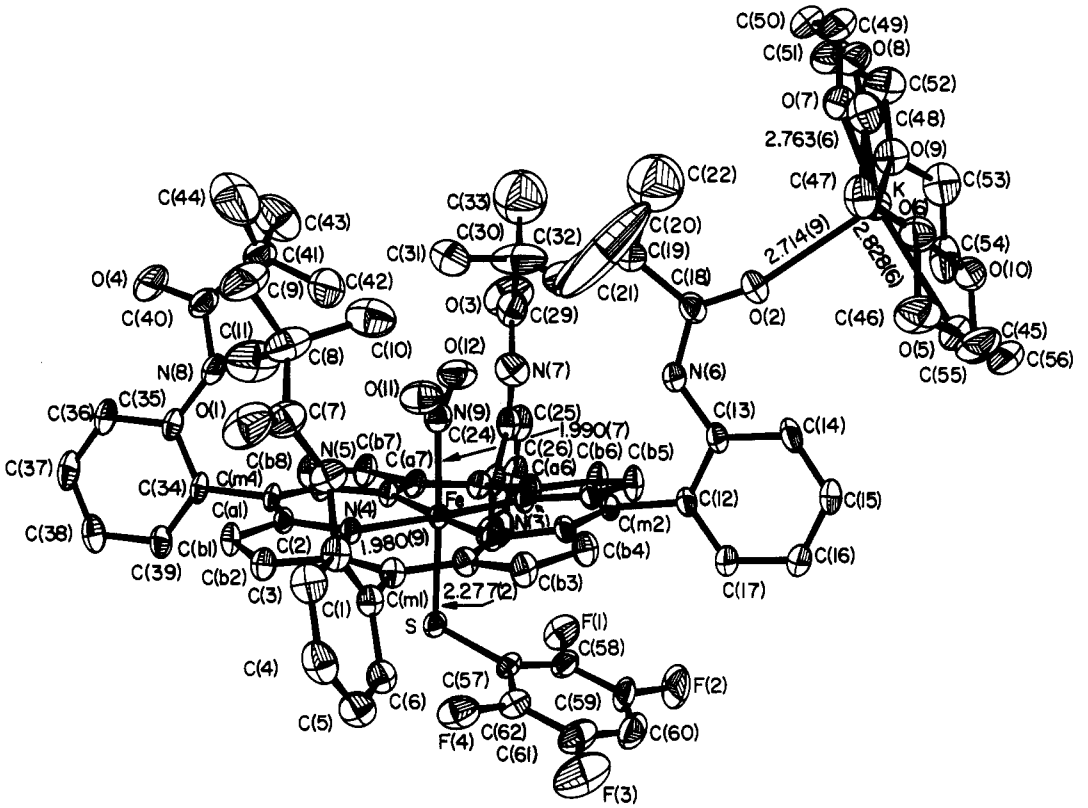

Figure 3. ORTEP diagram illustrating the structure of [K(18C6)][Fe(NO_2)(SC_6HF_4)(TpivPP)]. 30% probability ellipsoids are shown. The atom labels assigned to the crystallographically unique atoms of the molecule are shown. The interaction of the potassium ion with a carbonyl oxygen atom of a picket is illustrated. Also shown are the values of the bond distances in the two coordination groups.

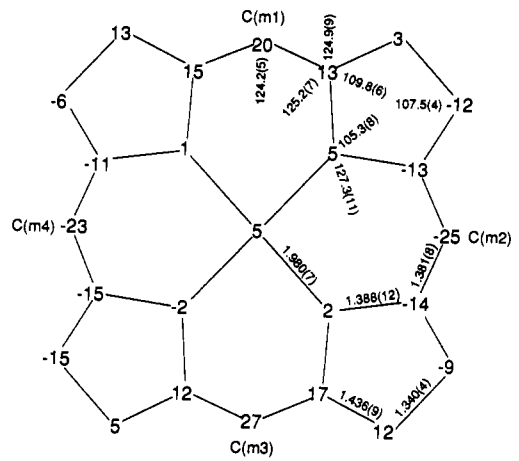

Figure 4. Formal diagram of the porphinato core of [Fe(NO_2)(SC_6HF_4)(TpivPP)]$^-$ illustrating the displacement of each unique atom (in units of 0.01 Å) from the mean plane of the 24-atom porphinato core. Positive values of the displacements are toward the axial thiolate ligand. Also displayed on the diagram is the averaged value of each type of bond distance and angle in the porphinato core.

plane of the six crown oxygen atoms toward the carbonyl oxygen. This coordination feature of the potassium ion has also been observed in another picket fence porphyrin structure ([Na(18C6)]-[Fe(SC_6F_4H)(TpivPP)]·C_6H_5Cl) where the distance C–O···Na is also a relatively short 2.33 Å.[25]

Averaged values of the bond distances and bond angles in the porphyrin core are shown in the formal diagram of Figure 4. Individual values of bond distances and angles are given in Tables SVI and SVII, respectively. Also displayed in Figure 4 are the deviations (in units of 0.01 Å) of the atoms from the mean plane of the 24-atom porphinato core. Figure 5 is a view normal to the porphyrin plane that shows the axial-ligand orientations and the disposition of the methyl carbon atoms of the pivaloyl pickets.

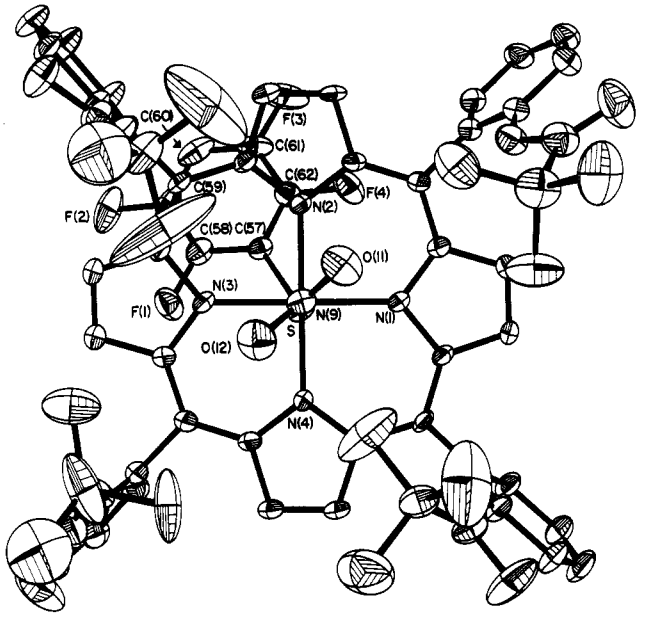

Figure 5. ORTEP diagram of the [K(18C6)][Fe(NO_2)(SC_6HF_4)(TpivPP) molecule viewed perpendicular to the mean plane of the porphinato core. The nitro ligand is closest to the viewer. The orientations of the pickets with respect to the nitro ligand are illustrated.

The angle between the nitro group plane and the closest Fe–N_p vector is 32°, while the angle between the nitro group plane and the FeSC(57) plane is 82°.

The EPR spectrum of crystalline [Fe(NO_2)(SC_6HF_4)-(TpivPP)]$^-$ shows that this complex has a rhombic, low-spin state. The spectrum of finely ground crystals of this material (recorded at 77 K) is a "normal" rhombic low-spin spectrum with $g_1 = 2.40$, $g_2 = 2.30$, and $g_3 = 1.91$. The EPR spectrum of frozen chlorobenzene solutions are virtually identical, with $g_1 = 2.39$, $g_2 =$

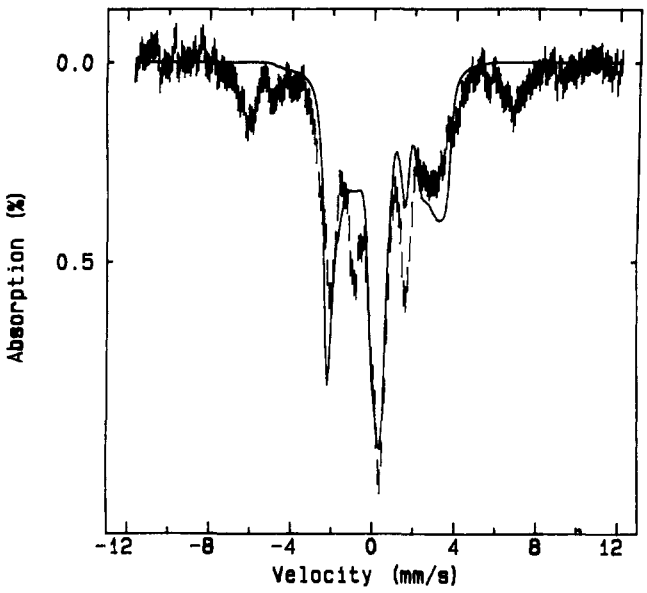

Figure 6. Mössbauer spectrum of [K(18C6)][Fe(NO_2)(SC_6HF_4)(TpivPP)]. The spectrum was recorded at 4.2 K with a magnetic field of 8 T applied parallel to the γ-beam. The solid line is a theoretical simulation using the parameters quoted in the text.

2.30, and $g_3 = 1.90$. Consistent with the EPR measurements, the room-temperature (295 K) Mössbauer spectrum of a crystalline sample of this compound shows a quadrupole doublet with parameters typical for low-spin ferric hemes. The quadrupole splitting, ΔE_q, is 2.12 mm/s, and the isomer shift, δ, is 0.22 mm/s. Mössbauer spectra recorded at liquid-helium temperature exhibit a complex magnetic pattern that is also characteristic for low-spin iron(III) hemes. Figure 6 shows a 4.2 K Mössbauer spectrum recorded in the presence of an 8-T magnetic field applied parallel to the γ-beam. The central magnetic component arises from the low-spin [Fe(NO_2)(SC_6HF_4)(TpivPP)]$^-$ complex. The observation of an additional spectral component with broad absorption peaks at -7.0 and $+7.5$ mm/s indicates that the sample (a collection of crystals) also contains $\sim 10\%$ of a high-spin ferric impurity ($S = {}^5/_2$). For the analysis of the low-spin ferric component, we use the following $S = {}^1/_2$ spin Hamiltonian to simulate theoretical spectra and compare the simulations with the experimental spectra:

$$\hat{H} = \beta\vec{S}\cdot\tilde{g}\cdot\vec{H} + \vec{S}\cdot\tilde{A}\cdot\vec{I} + \frac{eQV_{zz}}{4}\left[I_z^2 - \frac{I(I+1)}{3} + \frac{\eta}{3}(I_x^2 - I_y^2)\right] - g_n\beta_n\vec{H}\cdot\vec{I} \quad (1)$$

In this analysis, the g values are determined from the EPR experiments. The principal components of the magnetic hyperfine coupling $\tilde{A}$ tensor are derived from the measured g values using a simple ligand field theory.[26] The values for ΔE_q and δ are estimated from the zero-field spectrum recorded at 4.2 K. They are respectively 2.30 and 0.28 mm/s. Consequently, the only free parameter in eq 1 is the asymmetry parameter η. In order for the theoretical spectra to resemble the experimental data, it is necessary to rotate the rhombic field axis system by an angle, α, of 45° about the z axis of the cubic field (which was defined as the direction along the principal axis having the maximum g value[27]). For such a rotation, the principal axes of the $\tilde{g}$ and $\tilde{A}$ tensors remain aligned with the rhombic field axes. The *solid line* plotted in Figure 6 is a theoretical simulation with the following parameters: $g_x = 1.91$, $g_y = 2.30$, $g_z = 2.40$, $A_{xx}/g_n\beta_n = -6.2$ T, $A_{yy}/g_n\beta_n = -33.3$ T, $A_{zz}/g_n\beta_n = 15.2$ T, $\delta = 0.28$ mm/s, $\Delta E_q = 2.30$ mm/s, $\eta = 2.2$, and $\alpha = 45°$.

Discussion

We first briefly consider the nitrosyl complex. We determined the structure of the crystalline complex in order to define the nature of the potassium 18-crown-6 species present in the lattice. In the event, the finding of a cocrystallized [K(18-crown-6)]$^+$ nitrite complex is the least interesting of the several possibilities we had envisioned. The structure of the eight-coordinate [K(18-crown-6)(NO_2)] complex is similar to that of two nitrate complexes[29,30] in which the nitrate ion is bidentate. The K^+ ion displacement out of the O_6 plane is larger in the nitrite complex, suggesting a somewhat stronger interaction with the axial nitrite ion.

The physical properties of [Fe(NO)(TpivPP)] are closely similar to those reported for "open" porphyrins and shows that the ligand-binding pocket has little or no effect on them. Thus, the solution EPR spectrum (both g values and ^{14}N hyperfine splitting) is quite similar to that reported by Wayland and Olson[23] for [Fe(NO)(TPP)]. The NO stretching frequency is ~ 1665 cm^{-1} (partially obscured by the carbonyl stretch of the porphyrin pickets), which is comparable to the 1670 cm^{-1} observed for [Fe(NO)(TPP)].[22] The axial Fe–N(NO) bond distance (1.716 (15) Å) is similar to those found previously in a series of five- and six-coordinate TPP complexes[22,31,32] and shows the same bent Fe–N–O group. The equatorial Fe–N_p distance of 1.981 Å is a bit shorter than those observed in previous nitrosyl complexes[22,31,32] and is attributable to ruffling in the core of [Fe(NO)(TpivPP)] (cf. Figure 2).

We observe that mixed-axial-ligand iron(III) porphyrinates such as the thiolate/nitrite complex [Fe(NO_2)(SC_6HF_4)(TpivPP)]$^-$ are relatively uncommon. Consequently, it is pertinent to ask which axial ligand, if either, dominates in the bonding of the mixed-axial-ligand complex [Fe(NO_2)(SC_6HF_4)(TpivPP)]$^-$. The necessity of rotating the $\tilde{g}$ and $\tilde{A}$ tensor axes[33] with respect to the ligand field axes in order to achieve reasonable fits of the magnetic Mössbauer spectra appears to be a relatively unusual requirement, although this rotation of the $\tilde{g}$ and $\tilde{A}$ tensors has been found necessary for other (nitro)iron(III) porphyrinate complexes.[4] We believe that the same physical interpretation we have given previously remains appropriate, namely that the orientations of the dπ (d_{yz}, d_{xz}) orbitals do not correspond to the directions that are usually taken from the heme geometry. Rather, the two orthogonal dπ orbitals are oriented between the Fe–N_p vectors, with their planes perpendicular to the heme plane. If such an orientation of the dπ orbitals is indeed correct, it must result from the orientation of the axial ligands. However, the approximately orthogonal orientation of the two axial ligands with respect to each other logically can allow either axial ligand to have controlled the dπ orbital orientation. The relatively high position of N-bound nitrite on the spectrochemical series suggests that it must be a good π-acceptor ligand.[34] Effective π bonding between iron and nitrite thus requires a filled dπ orbital with lobes perpendicular to the nitrite plane. The sulfur atom of the thi-

(26) Oosterhuis, W. T.; Lang, G. *Phys. Rev.* **1969**, *178*, 439.
(27) We note that in this analysis we have assumed that the principal magnetic direction (conventionally taken as z) corresponds to the heme normal. This assumption has been verified for other (nitro)iron(III) complexes by single-crystal EPR measurements.[28]
(28) Lloyd, S.; Huynh, B. H.; Nasri, H.; Scheidt, W. R. Work in progress.
(29) Dyer, R. B.; Ghirardelli, R. G.; Palmer, R. A.; Holt, E. M. *Inorg. Chem.* **1986**, *25*, 3184.
(30) Battaglia, L. P.; Corradi, B.; Bianchi, A.; Giusti, J.; Paoletti, P. *J. Chem. Soc., Dalton Trans.* **1987**, 1179.
(31) Piciulo, P. L.; Scheidt, W. R. *J. Am. Chem. Soc.* **1976**, *98*, 1913.
(32) Scheidt, W. R.; Brinegar, A. C.; Ferro, E. B.; Kirner, J. F. *J. Am. Chem. Soc.* **1977**, *99*, 7315.
(33) For simplicity we have used $\alpha = 45°$ to retain the alignment of the principal axes of the $\tilde{g}$ and $\tilde{A}$ tensors. Rotations with other values of α (except 0° and multiples of 45°) will result in the misalignment of the two axis systems. For further details on the effect of α, see ref 26.
(34) The importance of π-bonding for nitrite ion with iron porphyrinates is given by the observation that a *single* nitrite ion leads to a low-spin iron(II) porphyrinate. A strong π-acceptor ligand is thus indicated. See ref 5.

Table IV. Comparison of Bond Parameters of Nitrite and Thiolate Derivatives

complex	Fe--N_p[a,b]	Fe--N(NO_2)[a]	Fe--S[a]	NO_2^- angle[c,d]	C–S–Fe–N_p[c,e]	spin state[g]	ref
$[Fe(NO_2)_2TpivPP)]^-$	1.992 (1)	2.001 (6)		37, 34		LS	3
$[Fe(NO_2)(Py)(TpivPP)]$	1.983 (3)	1.960 (5)		37		LS	4
$[Fe(NO_2)(HIm)(TpivPP)]$	1.970 (4)	1.949 (10)		37		LS	4
$[Fe(NO_2)(TpivPP)]^-$[f]	1.970 (4)	1.849 (6)		40		LS	5
$[Fe(NO_2)(SC_6HF_4)(TpivPP)]^-$	1.980 (7)	1.990 (7)	2.277 (2)	41	32	LS	this work
$[Fe(SPh)_2(TPP)]^-$	2.008 (7)		2.336 (2)		3	LS	35
$[Fe(SC_6HF_4)_2(TPP)]^-$	1.998 (3)		2.309 (1)		2	LS	36
			2.316 (1)		6		
$[Fe(O_2)(SC_6HF_4)(TpivPP)]^-$[f]	1.994 (4)		2.367 (3)		~0[h]	LS	21
[Fe(SPh)(TPP)]	2.063 (11)		2.315 (2)		2	HS	37
[Fe(SPhBr)(TPP)]	2.06 (10)		2.290 (2)		18	HS	37
$[Fe(SPhNO_2)(PP\ IX\ DME)]$	2.064 (18)		2.324 (2)		42	HS	38
[Fe(SPh)(OEP]	2.057 (6)		2.299 (3)		24	HS	39
$[Fe(SC_6HF_4)(TPP)]$	2.06 (4)		2.298 (5)		19	HS	40
$[Fe(SEt)(TpivPP)]^-$[f]	2.074 (10)		2.324 (2)		16	HS	41
$[Fe(SC_6HF_4)(TpivPP)]^-$[f]	2.076 (20)		2.370 (3)		~0[h]	HS	25

[a] Distances in angstroms. [b] Averaged value. [c] Value in degrees, calculated from reported coordinates. [d] NO_2^- angle is the dihedral angle between the NO_2^- plane and the closest Fe–N_p vector. [e] Unsigned dihedral angle. [f] Iron(II) derivative. [g] LS = low spin; HS = high spin. [h] Estimated; no coordinates given.

Table V. EPR Parameters for Low-Spin [K(18C6)][Fe(TpivPP)(NO_2)(SC_6HF_4)] and Several Related Systems

complex	g_z	g_y	g_x	V/λ[a]	Δ/λ[b]	V/Δ[c]	a[d]	b[e]	c[f]	sum[g]	ref
[Fe(CN)(Py)(TPP)]	3.31	1.76	0.34	0.66	2.07	0.32	0.824	0.483	0.231	0.9657	48
cytochrome *c*	3.06	2.25	1.25	1.48	2.56	0.58	0.932	0.318	0.175	0.9998	42
$[Fe(HIm)_2(TPP)]ClO_4$	2.916	2.313	1.551	1.99	3.13	0.64	0.964	0.252	0.140	1.0123	43a
	2.988	2.271	1.480	1.79	3.16	0.56	0.956	0.274	0.144	1.0107	43b
$[Fe(NO_2)(Py)(TpivPP)]$	2.98	2.37	1.35	1.71	2.32	0.74	0.946	0.288	0.180	1.0100	4
$[Fe(NO_2)(HIm)(TpivPP)]$	2.87	2.34	1.56	2.09	2.94	0.71	0.964	0.242	0.144	1.0092	4
$[Fe(NO_2)_2(TpivPP)]^-$	2.67	2.49	1.57	2.57	1.92	1.34	0.963	0.205	0.172	0.9987	4
$[Fe(NO_2)(SC_6HF_4)(TpivPP)]^-$	2.40	2.30	1.91	5.10	4.01	1.27	0.995	0.104	0.083	1.0073	this work
cytochrome P-450	2.45	2.26	1.91	4.59	5.11	0.90	0.995	0.114	0.074	1.0088	44
cytochrome P-450 (2-PhIm)	2.41	2.25	1.91	4.91	5.04	0.97	0.994	0.107	0.073	1.0037	45
$[Fe(SPh)_2(TPP)]^-$	2.336	2.215	1.962	6.35	6.49	0.98	0.999	0.082	0.056	1.0098	46
$Mb(Fe^{3+})N_3$	2.80	2.22	1.72	2.40	4.74	0.51	0.977	0.210	0.097	1.0082	49

[a] $V/\lambda = E_{yz} - E_{xz} = g_x/(g_z + g_y) + g_y/(g_z - g_x)$. [b] $\Delta/\lambda = E_{xz} - E_{xy} - (1/2)V/\lambda = g_x/(g_z + g_y) + g_z/(g_y - g_x) - (1/2)V/\lambda$ = tetragonality of Blumberg and Peisach.[50] [c] V/Δ = rhombicity of Blumberg and Peisach;[50] $V/\Delta \leq 2/3$ for a "proper" axis system.[47] [d] Orbital-mixing coefficient for d_{yz}. [e] Orbital-mixing coefficient for d_{xz}. [f] Orbital-mixing coefficient for d_{xy}. [g] Sum = $(a^2 + b^2 + c^2)$; theoretical value = 1.000.

olate ligand, on the other hand, with its filled valence shell is expected to be a π-donor and should then donate into the half-filled $d\pi$ orbital of low-spin iron(III). The perpendicular relative orientation of the two ligands (cf. Figure 5) is thus most appropriate for the two types of metal–ligand π bonding.

Table IV provides a tabulation of structural parameters of previously reported (porphinato)iron nitrite[3-5] and thiolate[25,35-41] complexes. Two different types of structural parameters need to be considered: the absolute orientation of the axial ligands with respect to the porphyrin coordinate system (conveniently defined by Fe–N_p vectors) and the coordination group bond distances. The nitrite ligand orientation can be defined as the dihedral angle between the closest Fe–N_p vector and the NO_2 plane; the values found are all close to bisecting an equatorial N_p–Fe–N_p angle. The orientation of thiolate ligands can be defined in terms of the (unsigned) C–S–Fe–N_p dihedral angle. The values for most thiolate derivatives are close to 0°, with all low-spin derivatives having such ligand orientations. The nitrite ligand orientation in $[Fe(NO_2)(SC_6HF_4)(TpivPP)]^-$ is seen to be closely similar to that in all other nitrite complexes. However, the thiolate ligand orientation in $[Fe(NO_2)(SC_6HF_4)(TpivPP)]^-$ is distinctly different from that of most thiolate derivatives of Table IV and especially those thiolate complexes with a low-spin state. It thus appears that the primary determinant of the absolute orientation of the nitrite and thiolate ligands is the nitro ligand. Finally, we note that steric interactions do not appear large enough to have any significant effects on axial-ligand orientation.

The axial-ligand bond distances do not appear to be greatly different from those of related species. The Fe–S distance is on the short end of those observed, while the axial nitrite distance in $[Fe(NO_2)(SC_6HF_4)(TpivPP)]^-$ is perhaps slightly longer than those found in the other mixed-ligand species of Table IV. Variations in the equatorial Fe–N_p distances for the low-spin derivatives of Table IV are related to porphinato core conformation; the shorter values for the nitro derivatives reflect the S_4-ruffled cores found for these species. On the whole, the bond distances are unremarkable.

Table V lists *g* values and derived parameters for a range of low-spin ferric porphyrinates, including $[Fe(NO_2)(SC_6HF_4)(TpivPP)]^-$. An analysis[47] of the EPR parameters for $[Fe(NO_2)(SC_6HF_4)(TpivPP)]^-$ and related complexes can be used

(35) Byrn, M. P.; Strouse, C. E. *J. Am. Chem. Soc.* **1981**, *103*, 2633.
(36) Doppelt, P.; Fischer, J.; Weiss, R. *Croat. Chem. Acta* **1984**, *57*, 507.
(37) Byrn, M. P.; Strouse, C. E. *J. Am. Chem. Soc.* **1991**, *113*, 2501.
(38) Tang, S. C.; Koch, S.; Papaefthymiou, G. C.; Foner, S.; Frankel, R. B.; Ibers, J. A.; Holm, R. H. *J. Am. Chem. Soc.* **1976**, *98*, 2414.
(39) Miller, K. M.; Strouse, C. E. *Acta Crystallogr., Sect. C* **1984**, *C40*, 1324.
(40) Miller, K. M.; Strouse, C. E. *Inorg. Chem.* **1984**, *23*, 2395.
(41) Schappacher, M.; Ricard, L.; Fischer, J.; Weiss, R.; Montiel-Montoya, R.; Bill, E. *Inorg. Chem.* **1989**, *28*, 4639.
(42) Mailer, C.; Taylor, C. P. S. *Can. J. Biochem.* **1972**, *50*, 1048.
(43) (a) Walker, F. A.; Huynh, B. H.; Scheidt, W. R.; Osvath, S. R. *J. Am. Chem. Soc.* **1986**, *108*, 5288. (b) Soltis, S. M.; Strouse, C. E. *J. Am. Chem. Soc.* **1988**, *110*, 2824.
(44) Tsai, R.; Yu, C.-A.; Gunsalus, I. C.; Peisach, J.; Blumberg, W.; Orme-Johnson, W. H.; Beinert, H. *Proc. Natl. Acad. Sci. U.S.A.* **1970**, *66*, 1157.
(45) Sharrock, M.; Debrunner, P. G.; Schulz, C.; Lipscomb, J. D.; Marshall, V.; Gunsalus, I. C. *Biochim. Biophys. Acta* **1976**, *420*, 8.
(46) Byrn, M. P.; Katz, B. A.; Keder, N. L.; Levan, K. R.; Magurany, C. J.; Miller, K. M.; Pritt, J. W.; Strouse, C. E. *J. Am. Chem. Soc.* **1983**, *105*, 4916.
(47) Taylor, C. P. S. *Biochim. Biophys. Acta* **1977**, *491*, 137.
(48) Inniss, D.; Soltis, S. M.; Strouse, C. E. *J. Am. Chem. Soc.* **1988**, *110*, 5644.
(49) Hori, H. *Biochim. Biophys. Acta* **1971**, *251*, 227.

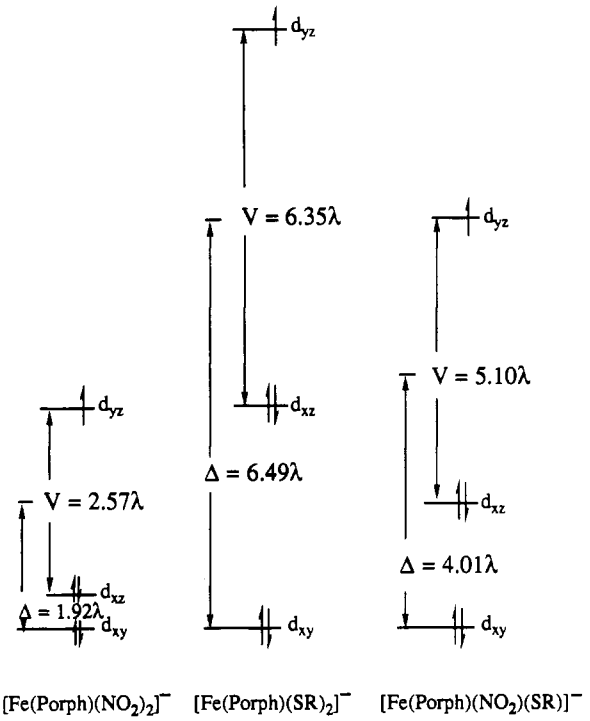

Figure 7. Schematic depiction of the ligand field parameters calculated from the EPR *g* values for bis(nitro), bis(thiolato), and the mixed (nitro)-(thiolato) complexes.

to qualitatively define ligand field energy parameters (in terms of the spin–orbit coupling constant, λ), as shown in Figure 7. Some interesting generalizations are apparent from the derived parameters. The bis(nitro)[3] and bis(thiolato)[46] complexes show the intrinsic effects of nitrite and thiolate ligands on the t_{2g} set of orbitals. Thiolate is seen to lead to much larger values of V/λ and Δ/λ than any other low-spin iron(III) porphyrinate species. Hence, pure thiolate ligation leads to much larger absolute splittings of V and Δ, unless the spin–orbit coupling constant λ is larger in the thiolates than in all other complexes (by a factor of at least 2, which would seem to be most unlikely). Nitrite coordination leads to a very large rhombicity (V/Δ)[50] and also a relatively large value of V/λ, consistent with its strong π-acceptor character. The thiolate surely makes a major contribution to the large values of V/λ and Δ/λ in the mixed nitro/thiolato ligand system, while both ligands of the pair must contribute to the large rhombicity. The large absolute values of V and Δ for the thiolate complexes must result from high polarizability of the sulfur donor and are not a measure of the intrinsic ligand field strength. Despite these large values of V and Δ in thiolate complexes, it is important to note that nitrite must be a much stronger field ligand than thiolate, since a five-coordinate (porphinato)iron(II) nitrite complex is low spin[5] while five-coordinate (porphinato)iron(II) thiolate complexes are high spin.[25,41] Nonetheless, as suggested by Blumberg and Peisach,[50] the empirical comparisons of tetragonalities and rhombicities are seen to remain useful for ligand identification. The value of such comparisons is readily seen from the EPR parameters of the cytochrome P-450 derivatives of Table V.

Although the presence of a nitrite ligand coordinated to an iron(III) porphyrinate clearly leads to a readily reduced iron complex (yielding an iron(II) nitrosyl product), mixed-ligand (thiolate/nitrite) iron(III) porphyrinate derivatives can be prepared. The bonding/electronic structure of the iron(III) atom in the resulting mixed-ligand, low-spin derivative appears to be largely dominated by the nitro ligand.

Acknowledgment. We are grateful for support of this research from the National Institutes of Health through Grant GM-38401 (W.R.S.) and the National Science Foundation through Grant DMB 9001530 (B.H.H.).

Supplementary Material Available: Table SI, giving complete crystallographic details for both complexes, Tables SII and SIII, listing anisotropic thermal parameters and fixed hydrogen atom positions for [K(18C6)][Fe(NO_2)(SC_6HF_4)(TpivPP)]·2C_6H_6·C_5H_{12}, Tables SIV and SV, giving isotropic and anisotropic thermal parameters and fixed hydrogen atom positions for [Fe(NO)(TpivPP)][K(NO_2)(18C6)]·$^1/_2C_6H_5Cl$, Tables SVI–SIX, listing bond distances and angles for both complexes, and Figure S1, showing an ORTEP drawing of the [K(NO_2)-(18C6)] complex in [Fe(NO)(TpivPP)][K(NO_2)(18C6)]·$^1/_2C_6H_5Cl$ (19 pages); listings of observed and calculated structure amplitudes (×10) for both complexes (57 pages). Ordering information is given on any current masthead page.

(50) Blumberg, W. E.; Peisach, J. *Adv. Chem. Ser.* **1971**, *100*, 271.